Structure-Based Design of Novel HIV-1 Protease Inhibitors To Combat Drug Resistance

Arun K. Ghosh,*,† Perali Ramu Sridhar,† Sofiya Leshchenko,† Azhar K. Hussain,† Jianfeng Li,† Andrey Yu. Kovalevsky,‖ D. Eric Walters,‡ Joseph E. Wedekind,‡,# Valerie Grum-Tokars,‡ Debananda Das,§ Yasuhiro Koh,⊥ Kenji Maeda,§ Hiroyuki Gatanaga,§ Irene T. Weber,‖ and Hiroaki Mitsuya⊥,§

Departments of Chemistry and Medicinal Chemistry, Purdue University, West Lafayette, Indiana 47907; Department of Biology, Molecular Basis of Disease, Georgia State University, Atlanta, Georgia 30303; Department of Biochemistry and Molecular Biology, Rosalind Franklin University of Medicine and Science, North Chicago, Illinois 60064; Departments of Hematology and Infectious Diseases, Kumamoto University School of Medicine, Kumamoto 860-8556, Japan; and Experimental Retrovirology Section, HIV and AIDS Malignancy Branch, National Cancer Institute, Bethesda, Maryland 20892

Received May 11, 2006

Structure-based design and synthesis of novel HIV protease inhibitors are described. The inhibitors are designed specifically to interact with the backbone of HIV protease active site to combat drug resistance. Inhibitor **3** has exhibited exceedingly potent enzyme inhibitory and antiviral potency. Furthermore, this inhibitor maintains impressive potency against a wide spectrum of HIV including a variety of multi-PI-resistant clinical strains. The inhibitors incorporated a stereochemically defined 5-hexahydrocyclopenta[*b*]-furanyl urethane as the P2-ligand into the (*R*)-(hydroxyethylamino)sulfonamide isostere. Optically active (3a*S*,5*R*,6a*R*)-5-hydroxy-hexahydrocyclopenta[*b*]furan was prepared by an enzymatic asymmetrization of meso-diacetate with acetyl cholinesterase, radical cyclization, and Lewis acid-catalyzed anomeric reduction as the key steps. A protein−ligand X-ray crystal structure of inhibitor **3**-bound HIV-1 protease (1.35 Å resolution) revealed extensive interactions in the HIV protease active site including strong hydrogen bonding interactions with the backbone. This design strategy may lead to novel inhibitors that can combat drug resistance.

Introduction

The AIDS epidemic is one of the most challenging problems in medicine in the 21st century.[1] Among many strategies to combat this disease, highly active antiretroviral therapy (HAART) with HIV protease inhibitors (PI) in combination with reverse transcriptase inhibitors continues to be the first line treatment for control of HIV infection.[2] This treatment regimen has definitely improved quality of life, enhanced HIV management, and halted the progression of the disease. Despite these impressive successes, there are serious limitations including major toxicity and complexity of these treatment regimens. Perhaps the most serious problem is that a growing number of patients are developing multi-drug-resistant strains of HIV, and there is ample evidence that these strains can be transmitted.[3,4] Thus far, no effective treatment options exist for these patients. In this context, our research emphasis has been to design nonpeptidyl inhibitors and optimize their potency against mutant strains resistant to currently approved PIs.

We recently designed and developed a number of protease inhibitors with remarkable antiviral potency and drug-resistance profiles.[5,6] As shown in Figure 1, inhibitor **1** (now known as TMC-114, or Darunavir) has shown unprecedented picomolar enzyme inhibitory activity and antiviral potency, favorable drug resistance profiles against multi-drug-resistant HIV and encouraging pharmacokinetic properties.[7,8] This inhibitor has recently been approved by the United States Food and Drug Administration for treatment of drug-resistant HIV.[9] A high-resolution X-ray crystal structure of **1**-bound HIV protease has now revealed critical molecular insight into interactions responsible for the observed resistance profiles.[10] Structural analysis revealed that close contact of inhibitor **1** with the main chains of the protease active site amino acids (Asp-29 and Asp-30) is critical to its potency and wide-spectrum activity against multi-PI-resistant HIV-1 variants. It appears that both P2- and P2′-ligands of inhibitor **1** are involved in extensive hydrogen bonding with the protein backbone. Interestingly, examination of X-ray structures of **1**-bound protein−ligand complexes of wild-type HIV protease and mutant HIV proteases also revealed only a small distortion in the backbone conformations.[10] This is also evident in the X-ray structures of a number of other HIV

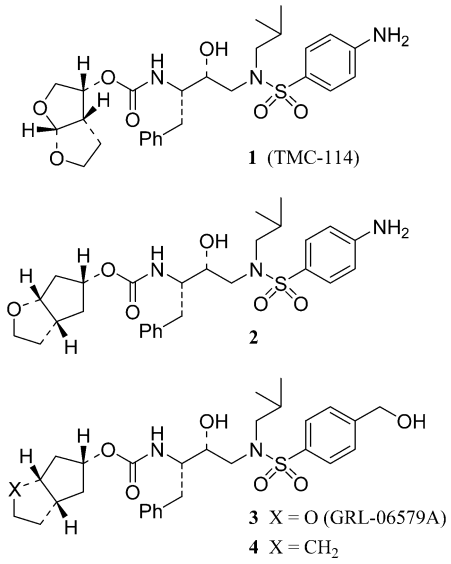

Figure 1. Structure of inhibitors **1**−**4**.

* Corresponding author. Phone (765)-494-5323. Fax (765) 496-1612. E-mail: akghosh@purdue.edu.
† Purdue University.
‖ Georgia State University.
‡ Rosalind Franklin University of Medicine and Science.
⊥ Kumamoto University School of Medicine.
§ HIV and AIDS Malignancy Branch, National Cancer Institute.
# Present address: Department of Biochemistry and Biophysics University of Rochester School of Medicine and Dentistry Rochester, NY 14642.

10.1021/jm060561m CCC: $33.50
Published on Web 08/02/2006

Scheme 1. Synthesis of Hexahydrocyclopenta[*b*]furanyl Carbonate

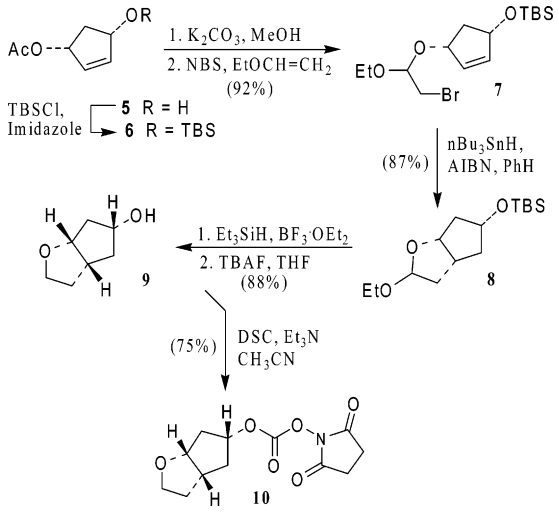

protease-inhibitor and related complexes.[11,12] Our working hypothesis to combat drug-resistance is to design inhibitors that make maximum interactions in the active site of HIV protease, particularly extensive hydrogen bonding interactions with the protein backbone in both S2- and S2′-sites. Conceivably, inhibitors exhibiting maximum hydrogen bonding interactions with the backbone of the wild-type enzyme may also retain potency against the mutant strains.

Upon the basis of this presumption, we have now designed and evaluated protease inhibitors (Figure 1) incorporating a novel ligand that can extensively interact with the backbone residues. The inhibitors incorporate a stereochemically defined bicyclic hexahydrocyclo-pentanofuran as the P2-ligand where the cyclic ether oxygen is positioned to hydrogen bond with the backbone Asp-29 NH. The bicyclic ligand is also expected to fill in the S2-subsite effectively. Furthermore, a 4-hydroxy-methylphenylsulfonamide is introduced as a P2′-ligand so that the hydroxyl group will be optimally positioned to hydrogen bond with the backbone residues in the S2′-subsite. Herein we report structure-based design, synthesis, preliminary biological evaluation, and X-ray crystal structure of inhibitor **3**-bound HIV-1 protease. The inhibitor has shown remarkable enzyme inhibitory and antiviral potency. Preliminary drug resistance profiles also indicated that the inhibitor maintains impressive potency against multi-PI-resistant clinical HIV-1 variants isolated from patients with drug-resistant HIV.

Chemistry

For synthesis of target inhibitors **2** and **3**, we devised an efficient synthetic route to (3a*S*,5*R*,6a*R*)-5-hydroxy-hexahydrocyclopenta[*b*]furan in optically active form. As shown in Scheme 1, enzymatic asymmetrization of meso-diacetate with acetyl cholinesterase provided the monoacetate **5** in multigram scale (85% yield).[13] Formation of Mosher ester of **5** revealed that enantiomeric purity of **5** was 95% ee.[14] Protection of hydroxyl group with TBSCl in the presence of imidazole in THF afforded TBS-ether **6**[15] in 98% yield. Hydrolysis of **6** with potassium carbonate in methanol gave the alcohol. Treatment of the resulting alcohol with ethyl vinyl ether and NBS in CH_2Cl_2 furnished bromo acetal **7**. Radical cyclization[16] of **7** with n-Bu_3-SnH in the presence of AIBN in benzene under reflux furnished bicyclic acetal **8** in excellent yield. Reduction of **8** with Et_3SiH in the presence of $BF_3.OEt_2$ followed by removal of TBS group with TBAF in THF afforded optically active hexahydrocyclo-

Scheme 2. Synthesis of P2-ligand and Active Carbonate

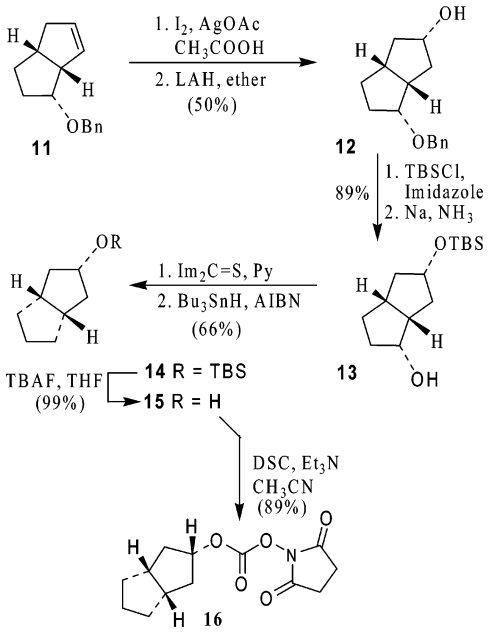

pentafuran-5-ol (**9**) in 88% yield. Treatment of **9** with *N*,*N*′-disuccinimidyl carbonate in the presence of Et_3N afforded mixed carbonate **10**.[17]

For the synthesis of inhibitor **4**, the corresponding P2-ligand, *endo-cis*-bicyclo[3.3.0]octan-3-ol was synthesized according to Scheme 2. Benzyl ether **11** was synthesized according to the literature procedure.[18] Exposure of **11** to iodine in the presence of silver acetate in acetic acid afforded the corresponding iodoacetate derivative.[19] Reduction of the resulting iodoacetate with LAH furnished hydroxy benzyl ether **12**[20] in 50% yield in two steps. The hydroxyl group in **12** was protected as TBS-ether by reaction with TBSCl and imidazole.[21] Subsequent removal of the benzyl ether with sodium in liquid ammonia[22] furnished hydroxyl TBS ether **13** in 89% yield. Removal of hydroxyl group in **13** was effected by using Barton−McCombie deoxygenation[23] reaction. Thus, alcohol **13** was reacted with *N*,*N*′-thiocarbonyldiimidazole in a mixture of (2:1) toluene and pyridine at 55 °C for 12 h. The resulting thiocarbonylimidazoyl derivative was treated with *n*Bu_3SnH in toluene at reflux to provide TBS ether **14** in 66% yield in two steps. Deprotection of TBS with TBAF in THF[21] furnished *endo-cis*-bicyclo[3.3.0]-octan-3-ol (**15**).[24] Treatment of alcohol **15** with *N*,*N*′-disuccinimidyl carbonate in the presence of Et_3N in acetonitrile afforded succinimidyl carbonate **16** in excellent yield.[17]

The synthesis of inhibitor **2** with hexahydrocyclopenta[*b*]-furanyl urethane as the P2-ligand and 4-aminosulfonamide as the P2′-ligand is shown in Scheme 3. Nitrosulfonamide derivative **18** was prepared from commercially available epoxide **17** as described previously.[25] Catalytic hydrogenation of **18** over 10% Pd/C in ethyl acetate for 11 h afforded the corresponding aminosulfonamide derivative.

Subsequent removal of Boc-group was effected by exposure of the resulting aminosulfonamide to trifluoroacetic acid in CH_2-Cl_2 to furnish the corresponding diamine. Selective alkoxycarbonylation of the aliphatic amine with succinimidyl carbonate **10** provided inhibitor **2** in 87% yield in the three-step sequence.

Synthesis of inhibitors **3** and **4** was carried out as shown in Scheme 4. For the preparation of hydroxyethylamine sulfonamide inhibitor scaffold, commercially available epoxide **17** was reacted with isobutylamine in 2-propanol. Treatment of the resulting amino alcohol with *p*-(diacetoxymethyl)phenylsulfonyl

Scheme 3. Synthesis of Inhibitor **2**

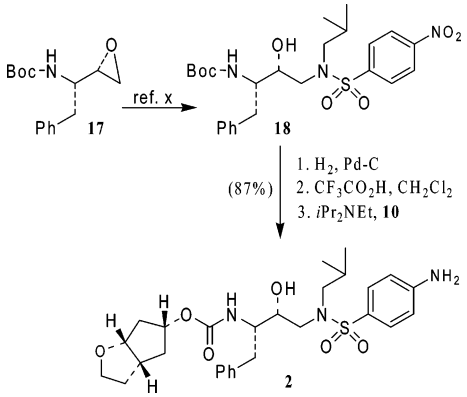

Scheme 4. Synthesis of Inhibitors **3** and **4**

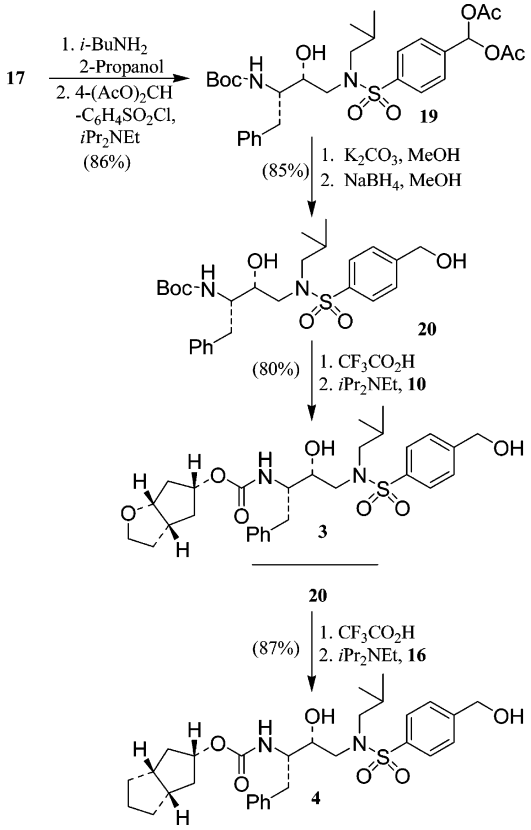

chloride[26] in the presence of diisopropylethylamine furnished sulfonamide derivative **19**. It was converted to hydroxymethylsulfonamide derivative **20** by deprotection of the acetates with K_2CO_3 and subsequent reduction of the resulting aldehyde with $NaBH_4$ in methanol. Sulfonamide derivative **20** was converted to inhibitor **3** by removal of Boc group by exposure to trifluoroacetic acid and reaction of the resulting amine with succinimidyl carbonate **10** and diisopropylethylamine in CH_2Cl_2. Inhibitor **2** was obtained in 80% yield. Similarly, reaction of the resulting amine with succinimidyl carbonate **16** afforded inhibitor **4** in 87% yield.

Results and Discussion

Inhibitors with hexahydrocyclopenta[*b*]furanyl urethane as the P2-ligand have shown impressive in vitro potency. Inhibitors **2**−**4** were evaluated in enzyme inhibitory and antiviral assays and the results are shown in Table 1. For enzyme inhibitory assay, we utilized the protocol described by Toth and Marshall[27]

Table 1. Enzyme Inhibitory and Antiviral Activity of Inhibitors

inhibitor[a]	K_i (nM)	IC_{50} (nM)
2	0.14 ±0.02	8
3	0.0045 ± 0.001	1.8
4	5.3 ± 0.3	>1000

[a]Inhibitor **1** has exhibited a K_i value of 14 pM and antiviral IC_{50} of 3 nM.

Table 2. Antiviral Data (IC_{50}) of **3** in PBMC and MT-2 Cells (nM)

virus	SQV	RTV	INV	NFV	APV	**3**
HIV-1_{LAI}[a]	14	43	32	14	34	1.8
HIV-1_{BA-L}[a]	18	36	24	7	29	2.0
HIV-1_{LAI}[b]	24	34	26	10	24	1.8
HIV-2_{EHO}[b]	1.9	290	13	20	440	21

[a] PBMC. [b] MT-2 cells; SQV (saquinavir), RTV (ritonavir), INV (indinavir), NFV (nelfinavir), APV (amprenavir); data represent the mean value of three determinations.

and the K_i-values denote the mean values of at least four determinations. As can be seen, inhibitor **2** which incorporates a stereochemically defined hexahydrocyclopenta[*b*]furanyl urethane as the P2-ligand and 4-aminosulfonamide as the P2′-ligand has shown enzymatic K_i value of 0.14 nM. As described previously, the X-ray crystal structure of protein−ligand complex of **1** and HIV-1 protease revealed that structural changes on the P2′-aryl ring could lead to improved interaction with the Asp-29 and Asp 30 NH.[10] In an effort to make the compound interact with backbone residues in the S2′-pocket more effectively, we incorporated a hydroxymethylsulfonamide derivative as the P2′-ligand in inhibitor **3**. This inhibitor exhibited a very impressive K_i value of 4.5 pM. To examine the importance of the ring oxygen of (*3aS*,*5R*,*6aS*)-5-hydroxy-hexahydro-cyclopenta[*b*]furanyl ligand in inhibitor **3**, the corresponding inhibitor **4** with an *endo*-3-bicyclo[3.3.0]octanyl urethane as the P2-ligand was evaluated. As shown, inhibitor **4** has shown an enzymatic K_i value of 5.3 nM, a >1100-fold reduction in potency compared to **3**. This marked difference in enzyme inhibitory potency is also reflected in their antiviral potency. Inhibitor **3** has shown an antiviral IC_{50} value of 1.8 nM in MT-2 human T-lymphoid cells exposed to HIV-1_{LAI}. Consistent with its enzyme inhibitory potency, inhibitor **2** has also shown good antiviral activity. In comparison, compound **4** has exhibited antiviral IC_{50} value of >1 μM, a drastic >500-fold reduction with respect to inhibitor **3**.

We have compared antiviral potency of inhibitor **3** against various FDA approved protease inhibitors. It has maintained a remarkable potency in MT-2 cells exposed to HIV-1_{LAI} compared to other FDA approved protease inhibitors. Antiviral activity against three different HIV isolates was determined in PHA-PBMC and MT-2 cells. The results are shown in Table 2. This inhibitor exerted far more potent activity against two HIV-1 isolates (HIV-1_{LAI} and HIV-1_{Ba-L}) in both MT-2 cells and PHA-PBMC than all currently available approved protease inhibitors examined. In addition, it was as potent against HIV-2_{EHO} as indinavir and nelfinavir with an IC_{50} value of 21 nM. In vitro cytotoxicity of inhibitor **3** was minimal and its concentration that reduced the viability of target cells by 50% (CC_{50}) was greater than 100 μM.

We also examined inhibitor **3** for its antiviral activity against a panel of multi-drug-resistant HIV-1 variants as shown in Table 3. An HIV-1 clinical strain HIV-1_{ET}, isolated from a drug-naïve patient with HIV-1 infection, was sensitive to all protease inhibitors examined, among which inhibitor **3** was most potent with the lowest IC_{50} value of 3 nM. In contrast, each of six drug-resistant clinical strains containing 10−12 protease inhibi-

Table 3. Activity of **3** against a Wide Spectrum of HIV-1 Variants[a]

virus	mutations[a]	IC_{50} (nM) values						
		SQV	RTV	IDV	NFV	APV	**1**	**3**
1 (ET)	L10I	17	15	30	32	23	nd	3
2 (B)	L10I,K14R,L33I,M36I,M46I,F53L,K55R,I62V,L63P,A71V, G73S,V82A,L90M,I93L	230	>1000	>1000	>1000	290	10.2	15
3 (C)	I10L,I15V,K20R,M36I,M46L,I54V,K55R,I62V,L63P,K70Q, V82A,L89M	100	>1000	500	310	300	3.5	5
4 (G)	L10I,V11I,T12E,I15V,L19I,R41K,M46L,L63P,A71T, V82A,L90M	59	>1000	500	170	310	3.7	20
5 (TM)	L10I,K14R,R41K,M46L, I54V,L63P,A71V,V82A,L90M, I93L	250	>1000	>1000	>1000	220	3.5	4
6 (EV)	L10V,K20R,L33F,M36I, M46I,I50V,I54V,D60E,L63P,A71V, V82A,L90M	>1000	>1000	>1000	>1000	>1000	nd	52
7 (ES)	L10I,M46L,K55R,I62V,L63P, I72L,G73C,V77I,I84V,L90M	>1000	>1000	>1000	>1000	>1000	nd	31
8 (K)	L10F/D30N/K45I/A71V/T74S	20	57	260	>1000	68	3	3

[a] Amino acid substitutions identified in the protease-encoding region of HIV-1_{ET} (ET), HIV-1_B (B), HIV-1_C (C), HIV-1_G (G), HIV-1_{TM} (TM), HIV-1_{EV} (EV), HIV-1_{ES} (ES), HIV-1_K (NFV_R) as compared to consensus B sequence cited from the Los Alamos database. All values were determined in triplicate. The IC_{50} values were determined by employing PHA-PBMC as target cells and the inhibition of $p24^{Gag}$ protein production as the endpoint.

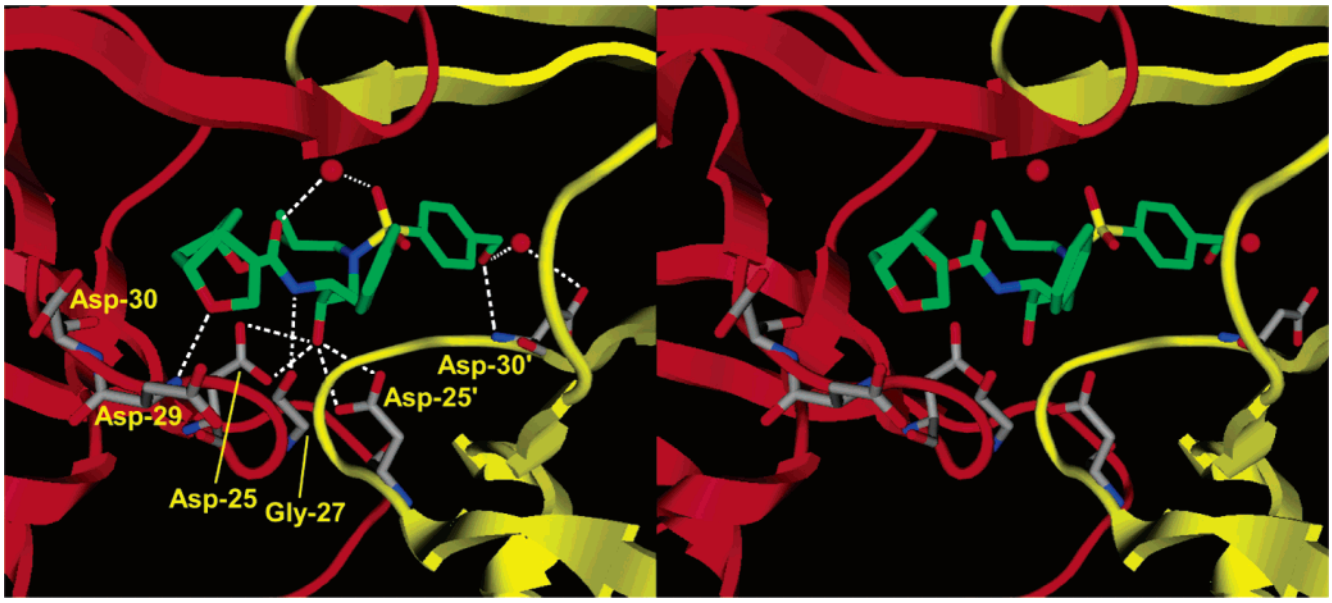

Figure 2. Stereoview of compound **3** bound to the active site of wild-type HIV-1 protease. The protein backbone is illustrated as a ribbon structure. Hydrogen bonds to the active site Asp-25 and Asp-25′, Gly-27, backbone NH of Asp-29, and Asp-30′, and to two bound water molecules are shown.

tor resistance-associated amino acid substitutions (HIV-1_B, HIV-1_C, HIV-1_G, HIV-1_{TM}, HIV-1_{EV}, and HIV-1_{ES}), isolated from patients with HIV-1 infection having received 7−11 different antiviral agents for 24 to 81 months,[5,7] was highly resistant to all the currently available protease inhibitors tested (Table 3). However, inhibitor **3** exerted highly potent activity against all of these six variants with IC_{50} values ranging 4−52 nM. An HIV-1 variant, HIV-1_K, which was selected in vitro in the presence of up to 5 μM concentrations of nelfinavir and contains five amino acid substitutions including D30N,[7] was also tested against inhibitor **3**. It was found that inhibitor **3** was highly potent against HIV-1_K with an IC_{50} value of as low as 3 nM (Table 3). These data indicate that inhibitor **3** is highly active against a wide spectrum of drug-resistant variants. Overall, the potency of inhibitor **3** against the HIV-1 strains tested in the present study was comparable to that of inhibitor **1**.

To gain molecular insight into the ligand-binding site interactions responsible for its potent antiviral activity against a wide spectrum of multi-PI-resistant HIV-1 variants, we have solved the X-ray crystal structure of the inhibitor complex with wild-type protease at 1.35 Å resolution.[28] A stereoview of the inhibitor **3**-bound structure is shown in Figure 2. The central hydroxyl group of the inhibitor forms four hydrogen bonds to the active site Asp25 and Asp25′ side chains, with the distances 2.6−3.2 Å. An oxygen of the sulfonamide group and the carbamate carbonyl oxygen form hydrogen bonds (2.8 and 2.9 Å, respectively) to the conserved water molecule that is hydrogen bonded to the backbone NH groups of Ile50 and Ile50′, as is commonly seen in HIV-1 protease/inhibitor complexes.[29] The oxygen of the P2 hexahydrocyclopentafuran forms a hydrogen bond with the backbone NH of Asp29 with the distance between heavy atoms of 2.8 Å.

This interaction cannot occur for inhibitor **4** which lacks the ring oxygen. The P2 hexahydrocyclopentafuranyl group also makes good C−H···O contacts with the main-chain carbonyl of Gly48. The amide nitrogen of the carbamate moiety has a 3.2 Å hydrogen bond with the main chain carbonyl oxygen of Gly27. The hydroxyl of the P2′ benzyl alcohol group forms a hydrogen bond to the backbone NH (3.1 Å) and a water-mediated contact with the side chain oxygen of Asp30 (OH_{inh}···H_2O···OOC distances are 2.5 and 2.3 Å, respectively). Therefore, the inhibitor **3** forms three direct hydrogen bonds and three water-mediated contacts to the protease residues, excluding contacts with catalytic aspartates. The important hydrophobic contacts include C−H···π interactions. The P1 benzyl group makes C−H···π interactions with Pro81′ and Val82′ (3.6−3.8 Å). The P1′ isobutyl group lies in a hydrophobic pocket formed by Pro81, Val82, Ile84, Gly49′, and Ile-

Table 4. Comparison of the Crystal Structure of Protease and Inhibitor **3** with Multi-PI-resistant Protease Crystal Structures[a]

PDB code	mutations	RMSD (Å)
2FDD[30]	L10I, K20R, M36I, M46I, I50V, I54V, I62V, L63P, A71V, V82A, L90M	0.7
1SGU[31]	K20R, L33F, M36I, I54V, L63P, A71V, V82A, I84V, L90M	0.5
1HSH[32]	L10V, M36I, M46I, A71V, I93L	1.1
2AZC[33]	M46I, F53L, L63P, V77I	0.8
1B6K[34]	K14R, R41K, L63P	0.5
2AVV[35]	L33I, G73S	0.5

[a] RMSD is the root-mean-square deviation of alpha-carbon positions for protease backbones.

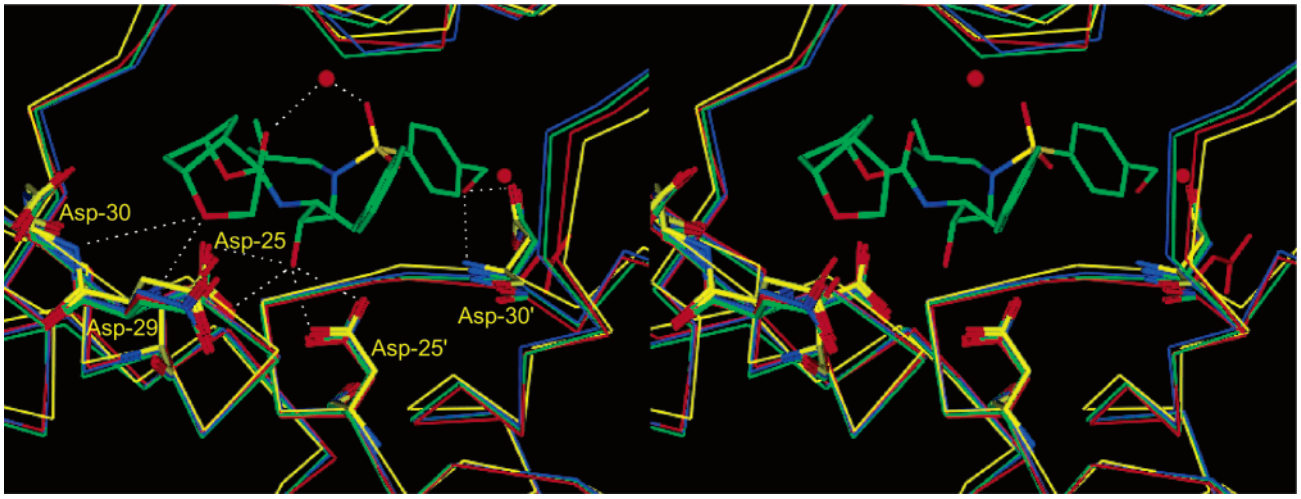

Figure 3. Stereoview of inhibitor **3** bound to the active site of wild-type HIV-1 protease, superimposed upon the structures of the three most highly mutated drug-resistant proteases of Table 3. Protein backbones are represented as alpha-carbon traces. Red = wild-type; blue = 2FDD; green = 1SGU; yellow = 1HSH. Note that, despite the multiple mutations, backbone positions change very little, especially in the active site, and hydrogen bonds to backbone NHs are not disrupted. Also, the hydroxymethyl is able to hydrogen bond to both the backbone and the side chain of Asp-30′.

50′. The P2′ group also forms a number of C−H···π contacts with Ala28′, Val32′, Ile47′, and Ile50, with distances of 3.6−3.9 Å with the closest interaction involving the side chain of Val32′. Inhibitor **3** participates in extensive interactions in the S2 to S2′ subsites, including tight hydrogen bonding with the protein backbone. Other PIs typically show fewer interactions with the main chain atoms. These interactions of inhibitor **3** with the protease backbone may explain its superior antiviral property and its potent activity against a wide spectrum of multi-PI-resistant HIV-1 strains.

To evaluate interactions of inhibitor **3** with the multi-drug-resistant variants of HIV-1 protease listed in Table 3, we have compared our crystal structure with several published crystal structures containing multiple mutations.[30−35] The structures used for comparison, and the relevant mutations, are listed in Table 4. None of these structures corresponds exactly to proteases of the multi-drug-resistant HIV-1 variants illustrated in Table 3, but these structures incorporate 21 of the 33 mutations listed in Table 3. The other mutations in Table 3 (V11I, T12E, I15V, L19I, M46L, K55R, D60E, K70Q, A71T, I72L, G73C, and L89M) have not, to our knowledge, been present in published crystal structures, with the exception of M46L. This mutation has been published only in unliganded crystal structures, in which the active site is open and distorted.[36,37] Residues 11, 12, 15, 19, 46, 55, 60, 70, 71, 72, 73, and 89 are all far from the active site, so that the effects of these mutations on drug resistance must be indirect and, therefore, difficult to model or predict. A stereoview of inhibitor **3** bound to the active site of wild-type HIV-1 protease, superimposed upon the structures of the three most highly mutated drug-resistant proteases (from Table 3), is shown in Figure 3.

In each case, a least-squares fit of protease alpha-carbons was carried out, and the interactions of inhibitor **3** with the mutant protease were examined. In all six structures, the following interactions were maintained: (a) hydrogen bonding of the secondary OH of the inhibitor to Asp-25 and Asp-25′ of the active site; (b) hydrogen bonding of the tetrahydrofuran oxygen of the inhibitor to the backbone NH of Asp-29, and a possible hydrogen bond to the backbone NH of Asp-30; (c) hydrogen bonding of the CH_2OH of the inhibitor to the backbone NH of Asp-30′; (d) hydrogen bonding of the CH_2OH of the inhibitor to the side chain carboxylate of Asp-30′ (requires ∼10−20° rotation of the side chain around the C-alpha:C-beta bond to optimize hydrogen bond distance; (e) in P2, van der Waals contact with Gly-48; (f) in P1, van der Waals contact with Gly-49, Ile-50, Leu-23′, and Pro-81′; (g) in P1′, van der Waals contact with Ile-84; (h) in P2′, van der Waals contact with Ile-50, Asp-30′, Val-32′, and Ile-47′.

Furthermore, many other binding interactions were also retained. These include: (a) in P2, van der Waals contact of Ile-47 was retained in all structures except 1HSH, which has the I47V mutation; van der Waals contact of Ile-50′ was retained in four of the structures, but was reduced in 2FDD (which has the I50V mutation) and in 2AZC; (b) in P1, van der Waals contact of Val-82′ was reduced in 2FDD, 1SGU, and 2AZC, all of which have the V82A mutation; van der Waals contact of Ile-84′ was retained in all structures except 1SGU, which has the I84V mutation; (c) in P1′, van der Waals contact of Pro-81 was reduced in 1HSH, 2AZC, and 1B6K; van der Waals contact of Val-82 was reduced in 2FDD, 1SGU, and 2AZC, all of which have the V82A mutation. All six were able to maintain binding to the water molecule in the binding site, with the exception of the 2AZC structure; as reported,[33] one of the flaps of this structure is distorted and a second water molecule is required for inhibitor binding to one of the Ile50 NH groups. It is noteworthy that, even in multi-drug-resistant

proteases with a number of mutations, the hydrogen bonding interactions of inhibitor **3** with the protease backbone are well maintained.

Conclusion

In summary, we have reported here the structure-based design of novel HIV-1 protease inhibitors incorporating a stereochemically defined 5-hexahydrocyclopenta[*b*]furanyl urethane as the P2-ligand and a 4-hydroxymethylsulfonamide as the P2′-ligand. The inhibitors are designed with the purpose of making extensive interactions including hydrogen bonding with the protein backbone of HIV-1 protease active site. One such inhibitor (**3**) has exhibited exceedingly potent antiviral activity and superior activity against multi-PI-resistant variants compared to other FDA approved PIs. The synthesis of P2-ligand alcohol, (3a*S*,5*R*,6a*R*)-5-hydroxy-hexahydrocyclopenta[*b*]furan was carried out enantioselectively by an enzymatic asymmetrization with acetyl cholinesterase as one of the key steps. A protein−ligand crystal structure of **3**-bound HIV-1 protease (1.35 Å resolution) revealed extensive interactions in the enzyme active site. Of particular note, both P2 and P2′-ligands are involved in hydrogen bonding with the backbone of both S2- and S2′-subsites. Comparison of protein−ligand X-ray structure of **3** with others structures of mutant proteases clearly indicated that the backbone interactions are maintained. The design of an inhibitor to specifically interact with the backbone may serve as an important guide to combat drug resistance. Further design and chemical modifications are currently underway.

Experimental Section

General. All moisture sensitive reactions were carried out under nitrogen or argon atmosphere. Anhydrous solvents were obtained as follows: THF, diethyl ether and benzene, distilled from sodium and benzophenone; dichloromethane, pyridine, triethylamine, and diisopropylethylamine, distilled from CaH_2. All other solvents were HPLC grade. Column chromatography was performed with Whatman 240−400 mesh silica gel under low pressure of 5−10 psi. TLC was carried out with E. Merck silica gel 60-F-254 plates. ^{1}H and ^{13}C NMR spectra were recorded on Varian Mercury 300 and Bruker Avance 400 and 500 spectrometers. Infrared spectra were recorded on a Mattson Genesis II FTIR instrument. Optical rotations were measured using a Perkin-Elmer 341 polarimeter.

(1*R*,4*S*)-(+)-4-(*tert*-Butyldimethylsilyloxy)-2-cyclopentenyl Acetate (6). To a stirred solution of alcohol **5** (1.1 g, 7.6 mmol) in tetrahydrofuran (20 mL) was added imidazole (779 mg, 11.4 mmol) followed by *tert*-butyldimethylsilyl chloride (1.54 g, 9.5 mmol). The reaction mixture was stirred at 23 °C for 24 h after which solids were removed by filtration, and the filtrate was concentrated to dryness. The residue was dissolved in ethyl acetate and washed with 1 N hydrochloric acid (3×), saturated aqueous sodium bicarbonate (2×), and brine solution. The organic phase was dried over anhydrous magnesium sulfate, filtered, and concentrated to give compound **6** (1.9 g, 99%) as a colorless liquid. ^{1}H NMR ($CDCl_3$, 300 MHz): δ 6.03 (m, 1H), 5.95 (m, 1H), 5.51 (m, 1H), 4.77 (m, 1H), 2.86 (dt, 1H, J = 7.5 Hz, J = 13.5 Hz), 2.10 (s, 3H), 1.66 (dt, 1H, J = 5 Hz, J = 14 Hz), 0.99 (s, 9H), 0.15 (s, 3H), 0.14 (s, 3H). ^{13}C NMR ($CDCl_3$, 75 MHz): δ 171.3, 139.3, 131.6, 77.4, 75.3, 41.6, 26.3, 21.6, 18.6, −4.1, −4.2.

1*R*,4*S*-[4-(2-Bromo-1-ethoxy-ethoxy)-cyclopent-2-enyloxy]-*tert*-butyl-dimethyl-silane (7). TBS-ether **6** (2 g, 7.8 mmol) was dissolved in methanol (50 mL) and treated with potassium carbonate (1.7 g, 12.5 mmol). The mixture was stirred for 20 min at 23 °C; solvent was evaporated under reduced pressure. The product was extracted with ethyl acetate (3×), dried over anhydrous sodium sulfate, and concentrated. The crude product was purified by flash column chromatography to provide hydroxyl ether (1.6 g, 97%) as a colorless oil. $[\alpha]^{20}_D$ −21.6 (*c* 1, $CHCl_3$) [lit.,[38] $[\alpha]^{20}_D$ −21.2 (*c* 0.89, $CHCl_3$)]; ^{1}H NMR ($CDCl_3$, 300 MHz): δ 5.84 (dd, J = 1 Hz, J = 9.0 Hz, 1H), 5.77 (dd, J = 1 Hz, J = 9 Hz, 1H), 4.56 (t, J = 9 Hz, 1H), 4. 48 (t, J = 9 Hz, 1H), 2.59 (dt, J = 12 Hz, J = 22 Hz, 1H), 2.40 (bs, 1H), 1.42 (dt, J = 7.5 Hz, J = 22 Hz, 1H). ^{13}C NMR ($CDCl_3$, 75 MHz): δ 137.0, 136.1, 75.6, 75.4, 44.9, 26.2, 18.5, −4.2.

To a solution of above hydroxyl ether (400 mg, 1.86 mmol) and *N*-bromosuccinimide (330 mg, 1.86 mmol) in CH_2Cl_2 (10 mL) at −10 °C was added ethyl vinyl ether (0.27 mL, 2.8 mmol). The reaction mixture was allowed to warm to 23 °C. After 12 h aqueous ammonium chloride (15 mL) was added and the layers were separated. The aqueous layer was extracted with CH_2Cl_2 (2×). Combined organic layers were washed with brine, dried over anhydrous sodium sulfate, and then concentrated in vacuo. The crude product was purified by flash column chromatography to afford compound **7** (660 mg, 97%) as a colorless liquid. ^{1}H NMR ($CDCl_3$, 300 MHz): 5.82 (d, 2H, J = 2.7 Hz), 4.70 (q, 1H, J = 5.7 Hz), 4.50−4.58 (m, 2H), 3.50−3.62 (m, 2H), 3.27−3.30 (m, 2H), 2.59−2.64 (m, 1H), 1.53−1.60 (m, 1H), 1.16−1.18 (m, 3H), 0.83 (s, 9H), 0.04 (s, 6H). ^{13}C NMR ($CDCl_3$, 75 MHz): 138.1, 138.0, 133.4, 133.0, 101.2, 101.0, 79.7, 79.6, 75.2, 75.1, 62.1, 61.9, 42.8, 42.3, 32.5, 32.4, 26.2, 26.0, 18.5, 15.6, 15.5, −4.1, −4.2. MS (CI): *m*/*z* 365.1 $[M + H]^+$; HRMS calcd for $C_{15}H_{29}BrO_3Si$ $[M + H]^+$ 365.1148; found 365.1145.

(3a*R*,5*R*,6a*R*)-2-Ethoxy-5-*tert*-butyldimethylsiloxy-hexahydro-cyclopenta[*b*]furan (8). The bromo derivative **7** (600 mg, 1.64 mmol), n-tributyltin hydride (0.6 mL, 2.14 mmol), and AIBN (10 mg) in benzene (15 mL) were refluxed for 4 h. Then it was cooled to 23 °C, and benzene was removed under reduced pressure. The crude product was chromatographed on silica gel to obtain bicyclic ether **8** (410 mg, 87%) as a viscous liquid. ^{1}H NMR ($CDCl_3$, 300 MHz): 5.86 (dd, 0.5 H, J = 2.4 Hz, J = 9.3 Hz), 5.12 (dd, 0.5 H, J = 4.5 Hz, J = 7.2 Hz), 3.97−4.75 (m, 2H), 3.63−3.74 (m, 1H), 3.32−3.40 (m, 1H), 2.22−2.78 (m, 1H), 1.52−2.04 (m, 4H). ^{13}C NMR ($CDCl_3$, 75 MHz): 106.1, 105.7, 83.1, 75.1, 73.6, 62.8, 62.6, 43.9, 42.6, 42.0, 41.5, 40.9, 40.2, 38.9, 38.9, 28.6, 27.1, 26.2, 26.1, 18.5, 18.3, 15.6, 15.5, −4.2, −4.4, −4.5. MS (CI): *m*/*z* 287.2 $[M + H]^+$; HRMS calcd for $C_{15}H_{30}O_3Si$ $[M + H]^+$ 287.2043: found 287.2041.

(3a*S*,5*R*,6a*R*)-5-Hydroxy-hexahydro-cyclopenta[*b*]furan (9). To a cold (0 °C) solution of bicyclic ether **8** (400 mg, 1.4 mmol) and triethylsilane (0.9 mL, 5.6 mmol) in CH_2Cl_2 (10 mL) was added $BF_3{\cdot}Et_2O$ (320 μL, 2.8 mmol), and the reaction mixture was stirred for 10 min. Saturated aqueous sodium bicarbonate solution (10 mL) was added, and the mixture was extracted with CH_2Cl_2 (3×). The combined extracts were dried over anhydrous sodium sulfate and concentrated in vacuo. Purification by flash column chromatography provided cyclopentanofuran derivative (300 mg, 90%) as a colorless liquid. $[\alpha]^{20}_D$ 8.6 (*c* 1, $CHCl_3$); ^{1}H NMR ($CDCl_3$, 300 MHz): δ 4.36 (m, 1H), 4.03 (m, 1H), 3.85 (m, 1H), 3.73 (m, 1H), 2.50 (m, 1H), 2.1−1.9 (m, 3H), 1.70 (m, 1H), 1.57 (m, 1H), 1.39 (m, 1H), 0.84 (s, 9H), 0.00 (s, 6H). ^{13}C NMR ($CDCl_3$, 75 MHz): δ 82.9, 73.6, 67.2, 42.8, 41.7, 40.9, 33.5, 26.2, 18.5, −4.3, −4.4. MS (CI): *m*/*z* 243.1 $[M + H]^+$; HRMS calcd for $C_{13}H_{26}O_2Si$ $[M + H]^+$ 243.1781; found 243.1779.

The above cyclopentanofuran (200 mg, 0.82 mmol) was dissolved in tetrahydrofuran (5 mL) and treated with tetrabutylammonium fluoride (1.2 mL, 1 M solution in tetrahydrofuran, 1.23 mmol). The mixture was stirred for 2 h at 23 °C. Solvent was removed under reduced pressure, and the crude product was purified by flash column chromatography to afford alcohol **9** (101 mg, 97%) as a viscous oil. $[\alpha]^{20}_D$ 13.0 (*c* 1, $CHCl_3$); ^{1}H NMR ($CDCl_3$, 300 MHz): δ 4.62 (dt, 1H, J = 1.2 Hz, J = 6.3 Hz), 4.47 (m, 1H), 4.27 (m, 1H), 3.85 (m, 1H), 2.90 (m, 1H), 1.5−2.6 (m, 7H). ^{13}C NMR ($CDCl_3$, 75 MHz): δ 86.0, 75.1, 68.6, 42.9, 41.8, 41.8, 35.4. MS (CI): *m*/*z* 129.1 $[M + H]^+$; HRMS calcd for $C_7H_{12}O_2$ $[M + H]^+$ 129.0916; found 129.0915.

(3a*S*,5*R*,6a*R*)-[Carbonic Acid 2′,5′-Dioxo-pyrrolidin-1-yl-ester]-hexahydro-cyclopenta[*b*]furan-5-yl Ester (10). A solution of alcohol **9** (50 mg, 0.39 mmol), *N*,*N*′-disuccinimidyl carbonate (122 mg, 0.47 mmol), and triethylamine (82 μL, 0.59 mmol) in acetonitrile (2 mL) was stirred at 23 °C for 12 h. After this period,

the reaction mixture was treated with saturated aqueous sodium bicarbonate (2 mL). The resulting mixture was extracted with ethyl acetate (3×). The combined organic extracts were dried over sodium sulfate. Evaporation of the solvent followed by flash column chromatography furnished mixed carbonate **10** (80 mg, 78%) as viscous oil. ^{1}H NMR ($CDCl_3$, 300 MHz): δ 5.23 (dt, 1H, J = 1.5 Hz, J = 5.7 Hz), 4.58 (m, 1H), 4.08 (m, 1H), 3.84 (m, 1H), 2.93 (s, 4H), 2.84 (m, 1H), 1.9−2.39 (m, 6H). ^{13}C NMR ($CDCl_3$, 75 MHz): δ 169.1, 151.3, 84.6, 83.5, 68.1, 41.9, 39.5, 38.4, 34.1, 25.8.

(±)-4-(Benzyloxy)-octahydropentalen-2-ol (12). To a suspension of benzyl ether **11** (500 mg, 2.47 mmol) and silver acetate (495 mg, 2.96 mmol) in acetic acid (6 mL) at 23 °C was added iodine (688 mg, 2.72 mmol) slowly for a period of 10 min. After being stirred for 2 h the reaction mixture was filtered and the filter cake was washed with CH_2Cl_2. The filtrate was concentrated under reduced pressure. The dark brown solution was diluted with CH_2Cl_2 washed with water, 2 N sodium carbonate solution, 5 N sodium thiosulfate solution, water, and brine solution, and dried over anhydrous sodium sulfate. The solvent was evaporated, and the crude product was purified by flash column chromatography to afford iodoacetate (690 mg, 70%) as a colorless liquid. ^{1}H NMR ($CDCl_3$, 300 MHz): δ 7.45−7.59 (m, 5H), 5.31−5.40 (dt, 1H, J = 9.9 Hz), 4.72−4.85 (ABq, 2H, υ = 20.7 Hz, J = 11.7 Hz, J = 29.7 Hz), 4.54 (t, 1H, J = 9 Hz), 4.09−4.15 (m, 1H), 3.07−3.15 (m, 1H), 2.65−2.70 (m, 1H), 2.24 (s, 3H), 2.20−2.23 (m, 1H), 1.78−1.90 (m, 2H), 1.56−1.63 (m, 1H), 1.26−1.37 (dt, 1H, J = 9.6 Hz). ^{13}C NMR ($CDCl_3$, 75 MHz): δ 170.9, 139.1, 128.7, 127.9, 127.8, 83.6, 80.2, 72.5, 54.4, 39.8, 37.0, 31.0, 28.9, 24.8, 21.4. MS (CI): m/z 401.0 $[M + H]^+$; HRMS calcd for $C_7H_{21}IO_3$ $[M + H]^+$ 401.0614; found 401.0611.

A solution of above iodoacetate (500 mg, 1.25 mmol) in diethyl ether (10 mL) was added to a suspension of lithium aluminum hydride (95 mg, 2.5 mmol) in diethyl ether (20 mL) at 0 °C. The mixture was heated at reflux for 24 h and then quenched by the addition of aqueous 4% sodium hydroxide solution (0.4 mL). The reaction mixture was stirred at room temperature for another 2 h. The white precipitate was filtered off, and the filtrate was evaporated to dryness in vacuo to give an oily residue which was purified by silica gel column chromatography to afford alcohol **12** (210 mg, 72%) as colorless oil. ^{1}H NMR ($CDCl_3$, 300 MHz): δ 7.43−7.47 (m, 5H), 4.73 (ABq, 2H, υ = 25.6 Hz, J = 11.7 Hz, J = 39.3 Hz), 4.32 (m, 1H), 4.11 (m, 1H), 3.92 (bs, 1H), 2.70−2.85 (m, 1H), 2.64−2.69 (m, 1H), 1.96−2.19 (m, 5H), 1.65−1.78 (m, 3H). ^{13}C NMR ($CDCl_3$, 75 MHz): δ 138.4, 128.8, 128.1, 82.0, 75.1, 71.6, 46.7, 42.4, 42.1, 35.5, 32.2, 31.2. MS (CI): m/z 233.1 $[M + H]^+$; HRMS calcd for $C_{15}H_{20}O_2$ $[M + H]^+$ 233.1542; found 233.1540.

(±)-5-(*tert*-Butyldimethylsilyloxy)-octahydropentalen-1-ol (13). To a solution of alcohol **12** (120 mg, 0.51 mmol) and imidazole (80 mg, 1.24 mmol) in dimethylformamide (3 mL) at 0 °C was added *tert*-butyldimethylsilyl chloride (92 mg, 0.61 mmol). The resulting mixture was stirred for 12 h at 23 °C. The reaction was quenched by addition of cold water (30 mL) and extracted with diethyl ether (3×). The combined organic extracts were dried over anhydrous sodium sulfate and filtered. Evaporation of the solvent followed by flash column chromatography of the crude product furnished TBS ether (160 mg, 90%) as colorless liquid. ^{1}H NMR ($CDCl_3$, 300 MHz): δ 7.18−7.28 (m, 5H), 4.43 (ABq, 2H, υ = 18.7 Hz, J = 12.0 Hz, J = 25.8 Hz), 3.95 (m, 1H), 4.77 (q, 1H, J = 7.2 Hz), 2.39 (m, 1H), 2.23 (m, 1H), 2.03 (m, 1H), 1.07−1.79 (m, 7H), 0.83 (s, 9H), 0.02 (s, 6H). ^{13}C NMR ($CDCl_3$, 75 MHz): δ 139.4, 128.7, 127.9, 127.7, 82.1, 74.8, 71.7, 43.8, 41.5, 38.1, 35.8, 29.2, 28.6, 26.3, 18.6, −4.2, −4.2. MS (CI): m/z 346.2 $[M + H]^+$; HRMS (m/z) $C_{21}H_{34}O_2Si$ $[M + H]^+$ 346.2328; found 346.2325.

To a stirred solution of sodium in liquid ammonia was added a solution of above TBS-ether (85 mg, 0.24 mmol) in THF (5 mL) dropwise for 5 min. The reaction was quenched by addition of excess solid ammonium chloride and allowed to warm to 23 °C. The mixture was diluted with water and extracted with CH_2Cl_2 (3×). The combined organic extracts were dried over anhydrous sodium sulfate. Evaporation of the solvent and flash column chromatography of the crude product furnished alcohol **13** (61 mg, 99%) as colorless liquid. ^{1}H NMR ($CDCl_3$, 300 MHz): δ 4.22 (m 1H), 3.97 (bs, 1H), 3.84 (bd, 1H, J = 9.3 Hz), 2.57−2.60 (m, 1H), 2.39−2.42 (m, 1H), 1.39−1.94 (m, 8H), 0.80 (s, 9H), 0.00 (s, 6H). ^{13}C NMR ($CDCl_3$, 75 MHz): δ 77.0, 74.4, 48.4, 43.4, 41.4, 38.1, 35.7, 31.7, 26.1, 18.4, −4.2, −4.8. MS (CI): m/z 257.1 $[M + H]^+$; HRMS calcd for $C_{14}H_{28}O_2Si$ $[M + H]^+$ 257.1936, found 257.1933.

(±)-*tert*-Butyldimethyl-(octahydropentalen1yloxy)silane (14). A solution of alcohol **13** (61 mg, 0.24 mmol) and *N*,*N*′-thiocarbonyldiimidazole (128 mg, 0.72 mmol) in 2:1 toluene−pyridine (6 mL) was heated at 55 °C for 12 h. After this period, the reaction mixture was concentrated in vacuo to a yellow residue which was dissolved in CH_2Cl_2 (20 mL) and washed with 0.1 N hydrochloric acid, saturated sodium bicarbonate solution, and then with water. The organic layer was dried over anhydrous sodium sulfate. Evaporation of solvent, followed by flash column chromatography yielded 1-*O*-thiocarbonyl imidazoyl derivative (70 mg, 82%) as colorless semisolid. ^{1}H NMR ($CDCl_3$, 300 MHz): δ 8.32 (s, 1H), 7.61 (s, 1H), 6.99 (s, 1H), 5.52−5.57 (m, 1H), 4.02−4.08 (m, 1H), 2.73−2.79 (m, 1H), 2.36−2.40 (m, 1H), 2.02−2.12 (m, 3H), 1.18−1.80 (m, 5H), 0.83 (s, 9H), 0.00 (s, 6H). ^{13}C NMR ($CDCl_3$, 75 MHz): δ 184.2, 137.3, 131.0, 118.3, 86.8, 74.8, 43.7, 42.0, 38.8, 36.1, 29.6, 28.5, 26.3, 18.6, −4.3, −4.2.

To a refluxing solution of tributyltinhydride (288 μL, 0.99 mmol) in dry toluene (5 mL) under argon atmosphere was added above thiocarbonylimidazoyl derivative (70 mg, 0.19 mmol) in dry toluene (5 mL) in a dropwise manner over 10 min. The reaction was refluxed for an additional 30 min, and the solvent was removed in vacuo to give colorless oil. The crude product was purified on a silica gel column to afford TBS ether **14** (40 mg, 80%) as a colorless oil. ^{1}H NMR ($CDCl_3$, 300 MHz): δ 3.95 (m, 1H), 2.24 (m, 2H), 1.91−1.96 (m, 2H), 1.11−1.59 (m, 8H), 0.83 (s, 9H), −0.01 (s, 6H). ^{13}C NMR ($CDCl_3$, 75 MHz): δ 75.0, 43.0, 40.1, 34.0, 29.0, 27.5, 26.3, 18.6, 16.2, 14.0, −4.3, −4.3. MS (CI): m/z 241.2 $[M + H]^+$; HRMS calcd for $C_{14}H_{28}OSi$ $[M + H]^+$ 241.2069; found 241.2061.

(±)-Octahydropentalen-2-ol (15). To a solution of TBS-ether **14** (30 mg, 0.11 mmol) in dry THF (1 mL) was added a 1 M solution of tetrabutylammonium fluoride (440 μL, 0.44 mmol), and the mixture was stirred at 23 °C for 10 h. After this period, solvent was removed under reduced pressure and the crude product was purified by flash chromatography to afford alcohol **15** (14 mg, 99%) as a colorless liquid. ^{1}H NMR ($CDCl_3$, 300 MHz): δ 4.06 (m, 1H), 2.33−2.36 (m, 2H), 2.11−2.16 (m, 2H), 1.54−1.66 (m, 4H), 1.42−1.45 (m, 2H), 1.14−1.18 (m, 2H). ^{13}C NMR ($CDCl_3$, 75 MHz): δ 74.3, 42.4, 40.0, 33.5, 29.6. MS (CI): m/z 127.1 $[M + H]^+$; HRMS calcd for $C_8H_{14}O$ $[M + H]^+$ 127.1124; found 127.1123.

Succinimidyl Carbonate 16. A solution of alcohol **15** (10 mg, 0.07 mmol), *N*,*N*′-disuccinimidyl carbonate (24.3 mg, 0.09 mmol), and triethylamine (14 μL, 0.1 mmol) in acetonitrile (2 mL) was stirred at 23 °C for 12 h. After this period, the solvent was evaporated and the residue was purified by flash column chromatography to afford the mixed carbonate **16** (15.3 mg, 89%) as a white solid. ^{1}H NMR ($CDCl_3$, 300 MHz): δ 4.88−4.95 (m, 1H), 2.76 (s, 4H), 2.35−2.37 (m, 2H), 2.13−2.23 (m, 2H), 1.59−1.66 (m, 2H), 1.35−1.49 (m, 6H). ^{13}C NMR ($CDCl_3$, 75 MHz): δ 169.1, 84.9, 40.6, 38.7, 34.1, 25.8.

Preparation of 4-Diacetoxytoluenesulfonyl Chloride. A solution of *p*-toluenesulfonyl chloride (4.02 g, 21.1 mmol) in a mixture (1:1) of acetic acid and acetic anhydride (80 mL) was treated with concentrated sulfuric acid (6.4 mL, 105.5 mmol) at 0 °C. Chromium trioxide (8 g, 84.4 mmol) was added slowly to maintain the reaction temperature below 10 °C. The mixture was stirred at 5 °C for 30 min. The reaction was quenched with ice water and filtered, and the solid filter cake was washed with water. The solid product was then suspended in saturated sodium bicarbonate solution, and the mixture was stirred for 2 h. The reaction mixture was extracted with ethyl acetate (3×). The combined organic layers were dried over anhydrous sodium sulfate. Evaporation of the solvent followed by purification of the resulting crude product by flash column chromatography provided the title compound (2.4 g, 38%) as a solid.

^{1}H NMR ($CDCl_3$, 300 MHz): δ 7.92 (d, 2H, J = 8.4 Hz), 7.79 (d, 2H, J = 8.4 Hz), 7.75 (s, 1H), 2.16 (s, 6H).

Compound 19. To a stirred solution of (1-oxiranyl 2-phenylethyl)-carbamate **17** (200 mg, 0.76 mmol) in 2-propanol (6 mL) was added isobutylamine (340 μL, 4.55 mmol). The resulting mixture was heated at reflux for 6 h. After this period, the reaction mixture was concentrated under reduced pressure and the residue was purified by flash column chromatography to provide the corresponding secondary amine (268 g, 99%) as a white solid. Mp 145 °C (decomposed); ^{1}H NMR ($CDCl_3$, 300 MHz): δ 7.20−7.33 (m, 5H), 4.69 (d, 1H, J = 8.8 Hz), 3.84−3.88 (m, 1H), 3.48−3.53 (m, 1H), 3.04 (dd, 1H, J = 4.5 Hz, J = 14.2 Hz), 2.90 (dd, 1H, J = 3.8 Hz, J = 7.8 Hz), 2.84 (dd, 1H, J = 3.1 Hz, J = 12.4 Hz), 2.76 (dd, 1H, J = 5.8, 12.3), 2.57 (dd, 1H, J = 6.6 Hz, J = 11.4 Hz), 2.44 (dd, 1H, J = 7 Hz, J = 11.7 Hz), 1.85−1.89 (m, 1H), 1.35 (s, 9H), 0.96 (d, 3H, J = 4.3 Hz), 0.95 (d, 3H, J = 4.3 Hz).^{13}C NMR (75 MHz, $CDCl_3$): δ 156.8, 137.8, 130.0, 128.9, 126.9, 80.3, 70.7, 57.9, 54.1, 52.2, 36.9, 28.7, 28.1, 20.9, 20.9. MS (ESI): m/z 359.2 $[M + Na]^+$; HRMS calcd for $C_{19}H_{32}N_2O_3$ $[M + Na]^+$; 359.2311; found 359.2306.

To a solution of above secondary amine (97 mg, 0.29 mmol) and 4-diacetoxytoluenesulfonyl chloride (103 mg, 0.35 mmol) in THF (5 mL) at 0 °C was added *N*,*N*′-diisopropylethylamine (78 μL, 0.45 mmol) followed by 4-(dimethylamino)pyridine (4 mg, 0.03 mmol). The resulting mixture was stirred at 23 °C for 4 h. Evaporation of the solvent under reduced pressure, followed by flash column chromatography over silica gel yielded compound **19** (151 mg, 88%) as an amorphous solid. ^{1}H NMR ($CDCl_3$, 300 MHz): δ 7.92 (d, 2H, J = 8.4 Hz), 7.81 (s, 1H), 7.76 (d, 2H, J = 8.4 Hz), 7.30−7.43 (m, 5H), 4.73 (d, 1H, J = 7.5 Hz), 3.84−3.92 (m, 2H), 3.20 (d, 2H, J = 6 Hz), 2.92−3.14 (m, 4H), 2.26 (s, 6H), 1.92−2.01 (m, 1H), 1.45 (s, 9H), 1.02 (d, 3H, J = 6.6 Hz), 0.98 (d, 3H, J = 6.6 Hz). ^{13}C NMR (75 MHz, $CDCl_3$): δ 169.0, 156.5, 140.4, 140.0, 138.1, 129.9, 128.9, 128.1, 128.0, 126.9, 88.9, 73.1, 58.8, 55.1, 54.0, 35.8, 28.6, 27.5, 21.2, 20.5, 20.2. MS (ESI): m/z 630.2 $[M + Na]^+$; HRMS calcd for $C_{30}H_{42}N_2O_9S$ $[M + Na]^+$ 630.2509: found 630.2504.

Compound 20. A solution of compound **19** (151 mg, 0.25 mmol) in methanol (10 mL) was treated with potassium carbonate (51 mg, 0.37 mmol). The mixture was stirred for 20 min at 23 °C. The solvent was evaporated under reduced pressure, and the product was extracted with ethyl acetate, dried over anhydrous sodium sulfate and concentrated. The crude product was purified by flash chromatography to provide the corresponding aldehyde (110 mg, 95%). ^{1}H NMR ($CDCl_3$, 300 MHz): 10.1 (s, 1H), 8.05 (d, 2H, J = 8.5 Hz), 7.99 (d, 2H, J = 8.5 Hz), 7.2−7.36 (m, 5H), 4.75 (d, 1H, J = 8.5 Hz), 3.81−3.94 (m, 3H), 3.22 (t, 2H, J = 3.5 Hz), 2.94−3.06 (m, 4H), 1.93 (m, 1H), 1.40 (s, 9H), 0.93 (d, 3H, J = 6.5 Hz), 0.91 (d, 3H, J = 6.5 Hz). ^{13}C NMR (75 MHz, $CDCl_3$): δ 191.2, 156.6, 144.4, 139.2, 138.1, 130.6, 129.9, 128.8, 128.4, 123.1, 80.3, 72.9, 58.3, 55.4, 53.4, 36.0, 28.6, 27.4, 20.4, 20.3. MS (ESI): m/z 527.2 $[M + Na]^+$; HRMS calcd for $C_{26}H_{36}N_2O_6S$ $[M + Na]^+$ 527.2192; found 527.2188.

To a stirred solution of above aldehyde (110 mg, 0.22 mmol) in methanol (2 mL) at 0 °C was added sodium borohydride (9.5 mg, 0.25 mmol), and the mixture was stirred for 15 min. The reaction was quenched with saturated ammonium chloride solution. The solvent was evaporated under reduced pressure, and the product was extracted with ethyl acetate (3×). The combined organic extracts were dried over anhydrous sodium sulfate, and solvent was evaporated. The crude product was purified by flash chromatography to provide compound **20** (96 mg, 90%) as an amorphous solid. ^{1}H NMR ($CDCl_3$, 300 MHz): δ 7.67 (d, 2H, J = 8.4 Hz), 7.43 (d, 2H, J = 8.4 Hz), 7.12−7.25 (m, 5H), 4.71 (s, 2H), 4.57 (d, 1H, J = 7.8 Hz), 3.67−3.76 (m, 3H), 2.72−3.03 (m, 6H), 1.78 (m, 1H), 1.27 (s, 9H), 0.83 (d, 3H, J = 6.6 Hz), 0.79 (d, 3H, J = 6.6 Hz). ^{13}C NMR ($CDCl_3$, 75 MHz): δ 156.4, 146.5, 138.1, 137.7, 129.9, 128.9, 127.9, 127.5, 126.8, 80.1, 73.1, 64.6, 59.0, 55.1, 54.0, 35.8, 28.6, 27.5, 20.5, 20.2. MS (ESI): m/z 529.2 $[M + Na]^+$; HRMS calcd for $C_{26}H_{38}N_2O_6S$ $[M + Na]^+$ 529.2349; found 529.2344.

Inhibitor 3. A solution of compound **20** (30 mg, 0.06 mmol) in 30% trifluoroacetic acid in CH_2Cl_2 (3 mL) was stirred at 23 °C for 30 min. After this period, the reaction mixture was concentrated under reduced pressure, and the residue was dissolved in toluene and evaporated at reduced pressure. The residue was dissolved in acetonitrile (2 mL) and cooled to 0 °C. To this solution were added *N*,*N*′-diisopropylethylamine (41 μL, 0.24 mmol) and mixed carbonate **10** (16.8 mg, 0.06 mmol). The resulting mixture was stirred at 23 °C for 6 h. The reaction mixture was concentrated under reduced pressure, and the residue was purified by flash chromatography over silica gel to furnish inhibitor **3** (28 mg, 87%) as an amorphous solid. ^{1}H NMR ($CDCl_3$, 300 MHz): δ 7.91 (d, 2H, J = 8.4 Hz), 7.66 (d, 2H, J = 8.4 Hz), 7.35−7.39 (m, 5H), 5.01 (t, 1H, J = 4.2 Hz), 4.93 (s, 2H), 4.89 (bs, 1H), 3.95−4.03 (m, 3H), 3.80−3.87 (m, 1H), 2.95−3.32 (m, 6H), 2.75−2.81 (m, 1H), 2.11−2.19 (m, 4H), 1.92−2.04 (m, 2H), 1.69−1.75 (m, 1H), 1.58 (dt, 1H, J = 4.5 Hz, J = 14.4 Hz), 1.08 (d, 3H, J = 6.6 Hz), 1.05 (d, 3H, J = 6.6 Hz). ^{13}C NMR ($CDCl_3$, 75 MHz): δ 156.6, 146.7, 137.9, 137.4, 129.8, 128.9, 127.9, 127.5, 126.9, 84.0, 77.4, 72.8, 68.1, 64.5, 59.1, 55.2, 54.1, 41.8, 39.7, 38.7, 36.2, 34.2, 27.6, 20.5, 20.2. MS (ESI): m/z 583.2 $[M + Na]^+$; HRMS calcd for $C_{29}H_{40}N_2O_7S$ $[M + Na]^+$ 583.2454; found 583.2465.

Inhibitor 4. A solution of compound **20** (23.4 mg, 0.05 mmol) in 30% trifluoroacetic acid in CH_2Cl_2 (3 mL) was stirred at 23 °C for 30 min. After this period, the reaction mixture was concentrated under reduced pressure and the residue was dissolved in toluene and evaporated. The residue was dissolved in acetonitrile (2 mL) and cooled to 0 °C. *N*,*N*′-Diisopropylethylamine (41 μL, 0.24 mmol) and mixed carbonate **16** (10.0 mg, 0.04 mmol) were then added. The resulting mixture was stirred for 6 h at 23 °C. The reaction mixture was then concentrated under reduced pressure, and the residue was purified by chromatography over silica gel to furnish inhibitor **4** (18 mg, 80%) as an amorphous solid. ^{1}H NMR ($CDCl_3$, 300 MHz): δ ^{1}H NMR ($CDCl_3$, 300 MHz): δ 8.00 (d, 2H, J = 8.4 Hz), 7.76 (d, 2H, J = 8.4 Hz), 7.45−7.57 (m, 5H), 5.04 (s, 2H), 4.96−5.00 (m, 1H), 4.06−4.14 (bm, 2H), 3.01−3.41 (m, 4H), 2.59 (m, 2H), 2.25−2.36 (m, 3H), 2.04−2.13 (m, 1H), 1.34−1.87 (m, 10H), 1.16 (d, 3H, J = 6.6 Hz), 1.12 (d, 3H, J = 6.6 Hz). ^{13}C NMR ($CDCl_3$, 75 MHz): δ 156.5, 146.5, 138.0, 137.6, 129.9, 128.9, 127.9, 127.5, 126.9, 73.0.4, 64.6, 59.0, 55.3, 54.0, 40.5, 39.2, 35.7, 34.1, 27.6, 25.7, 20.5, 20.2. MS (ESI): m/z 581.2 $[M + Na]^+$; HRMS calcd for $C_{30}H_{42}N_2O_6S$ $[M + Na]^+$ 581.2656; found 581.2663.

Inhibitor 2. To a solution of compound **18** (128 mg, 0.24 mmol) in ethyl acetate (15 mL) was added 10% Pd/C (10 mg). The mixture was stirred at 23 °C under an H_2-filled balloon for 11 h. The reaction mixture was filtered through a bed of Celite, and the filter cake was washed with ethyl acetate. Evaporation of solvent under reduced pressure, followed by flash chromatography on silica gel, afforded the corresponding aromatic amine (122 mg, 95%) as a white solid. M.p.: 60−63 °C; ^{1}H NMR ($CDCl_3$, 300 MHz): δ 7.54 (d, 2H, J = 8.5 Hz), 7.19−7.30 (m, 5H), 6.68 (d, 2H, J = 8.5 Hz), 4.60 (d, 1H, J = 8.4 Hz), 3.75−3.80 (m, 2H), 2.99−3.11 (m, 3H), 2.89−2.92 (m, 2H), 2.77 (dd, 1H, J = 6.7 Hz, J = 13.2 Hz), 1.80−1.86 (m, 1H), 1.34 (s, 9H), 0.89 (d, 3H, J = 6.6 Hz), 0.86 (d, 3H, J = 6.6 Hz). ^{13}C NMR ($CDCl_3$, 75 MHz): δ 156.0, 150.3, 137.9, 129.5, 128.4, 126.4, 114.3, 79.6, 72.8, 58.7, 54.6, 53.8, 35.4, 29.7, 28.2, 27.2, 20.2, 19.9. MS (ESI): m/z 514.2 $[M + Na]^+$; HRMS calcd for $C_{25}H_{37}N_3O_5S$ $[M + Na]^+$ 514.2352; found 514.2349.

A solution of above amine (22 mg, 0.04 mmol) in 30% trifluoroacetic acid in CH_2Cl_2 (3 mL) was stirred at 23 °C for 40 min. After this period, the reaction mixture was concentrated under reduced pressure and the residue was dissolved in acetonitrile (2 mL). The solution was cooled to 0 °C, and mixed carbonate **10** (11.5 mg, 0.04 mmol) and *N*,*N*′-diisopropylethylamine (43.8 μL, 0.25 mmol) were added. The resulting mixture was stirred at 23 °C for 8 h. The reaction mixture was then concentrated under reduced pressure, and the residue was purified by flash column chromatography over silica gel to provide inhibitor **2** (18.5 mg, 75%) as an amorphous solid. ^{1}H NMR ($CDCl_3$, 300 MHz): δ 7.58

(d, 2H, $J = 8.6$ Hz), 7.22−7.33 (m, 5H), 6.71 (d, 2H, $J = 8.6$ Hz), 4.91 (m, 1H), 4.79 (m, 1H), 4.43 (m, 1H), 3.87 (m, 2H), 3.71 (q, 1H, $J = 7$H), 3.01−3.16 (m, 2H), 2.93 (dd, 1H, $J = 8.2$ Hz), 2.86 (dd, 1H, $J = 8.6$ Hz, $J = 14.1$ Hz), 2.80 (dd, 1H, $J = 6.1$ Hz), 2.66 (m, 1H), 2.04 (m, 3H), 1.87 (m, 2H), 1.65 (m, 3H), 1.48 (m, 1H), 0.95 (d, 3H, $J = 6.5$ Hz), 0.90 (d, 3H, $J = 6.5$ Hz). ^{13}C NMR ($CDCl_3$, 75 MHz): δ 150.3, 137.4, 129.2, 128.1, 126.1, 125.9, 113.8, 83.4, 72.3, 67.4, 58.6, 54.5, 53.6, 41.2, 39.0, 38.1, 35.5, 33.6, 29.4, 27.0, 19.9, 19.6. MS (ESI): *m*/*z* 568.2 $[M + Na]^+$; HRMS calcd for $C_{28}H_{39}N_3O_6S$ $[M + Na]^+$ 568.2458; found 568.2461.

Cells, Viruses, and Antiviral Agents. MT-2 cells were grown in an RPMI-1640-based culture medium supplemented with 15% fetal calf serum (HyClone Laboratories, Logan, UT), 50 unit/mL penicillin, and 50 μg/mL of streptomycin. The following HIV-1 viruses were used for the drug susceptibility assay: HIV-1_{LAI}, HIV-1_{Ba-L}, and HIV-2_{EHO}.[7,9] 3′-Azido-2′,3′-dideoxythymidine (AZT or zidovudine) was purchased from Sigma (St. Louis, MO). Saquinavir (SQV) and ritonavir (RTV) were kindly provided by Roche Products Ltd. (Welwyn Garden City, U.K.) and Abbott Laboratories (Abbott Park, Ill.), respectively. Indinavir (IDV) and Nelfinavir (NFV) were kindly provided by Japan Energy Inc., Tokyo. Amprenavir (APV) was a kind gift from Glaxo-Wellcome, Research Triangle, NC.

Drug Susceptibility Assay. The susceptibility of HIV to various drugs was determined as previously described[7,9] with minor modifications. Briefly, MT-2 cells (2×10^4/mL) were exposed to 100 50% tissue culture infectious doses ($TCID_{50}$) of HIV in the presence of various concentrations of drugs in 96-well microculture plates and were incubated at 37 °C for 7 days. After 100 μL of the medium was removed from each well, 3-(4,5 dimethylthiazol-2-yl)-2,5-diphenyltetrazolium bromide (MTT) solution (10 μL, 7.5 mg/mL in phosphate-buffered saline) was added to each well in the plate, followed by incubation at 37 °C for 2 h. After incubation, to dissolve the formazan crystals, 100 μL of acidified 2-propanol containing 4% (v/v) Triton X-100 was added to each well and the optical density measured in a kinetic microplate reader (Vmax, Molecular Devices, Sunnyvale, CA). All assays were performed in duplicate or triplicate. In determining the sensitivty of HIV isolates to drugs, phytohemagglutinin-activated peripheral blood mononuclear cells (PHA-PBM) (1×10^6/mL) were exposed to 50 $TCID_{50}$ of each isolate and cultured in the presence or absence of various concentrations of drugs in 10-fold serial dilutions in 96-well microculture plates. On day 7 of culture, the supernatant was harvested and the amount of p24 Gag protein was determined by using a fully automated chemiluminescent enzyme immunoassay system (Lumipulse F; Fujirebio Inc., Tokyo).[7,9] Drug concentrations that suppressed the production of p24 Gag protein by 50% (IC_{50}) were determined by comparison with the p24 production level in drug-free control cell culture. All assays were performed in triplicate.

Determination of X-ray Structure of Inhibitor 3-Bound HIV Protease$_{WT}$. The X-ray crystal structure of inhibitor **3** bound to HIV Protease$_{WT}$ has been deposited in the Protein Databank with access code 2HB3. The crystals of the PR_{WT} complexed with GRL-06579A, which was dissolved in dimethyl sulfoxide, were grown by the hanging-drop vapor diffusion method using 10:1 molar ratio of the inhibitor to protein. The well solution contained sodium acetate buffer (pH = 4.2) and 1.4 M NaCl. Crystals were transferred into a cryoprotectant solution containing the reservoir solution plus 20−30% (v/v) glycerol, mounted on a nylon loop, and flash-frozen in liquid nitrogen. X-ray diffraction data were collected on the ×26C beamline of the National Synchrotron Light Source, Brookhaven National Laboratory at 90 K using 0.96 Å wavelength. Data were processed using HKL2000.[39] A medium-sized platelike crystal, with dimensions of 0.2 × 0.2 × 0.1 mm, diffracted to 1.35 Å resolution with mosaicity of 0.4° and produced an R_{sym} value of 5.0% (52%) for data between 50 and 1.35 Å resolution. These data were reduced in space group $P2_12_12$ with unit cell dimensions of $a = 58.1$ Å, $b = 86.5$, $c = 45.9$ Å with one dimer per asymmetric unit. The CPP4i suite of programs[40,41] was used to obtain a molecular replacement solution using as the starting model the PR_{L90M} complex with TMC114 (PDB code 2F81), which is in the same space group. The structure was refined using SHELX97[42] and refitted using O 10.[43] Alternate conformations were modeled for the protease residues when obvious in the electron density maps. Anisotropic atomic displacement parameters (*B*-factors) were refined for all atoms including solvent molecules. Stereochemical parameters for the inhibitor were created using GAUSSIAN03 with the DFT quantum-chemical method. Hydrogen atoms were added at the final stages of the refinement. The identity of ions and other solvent molecules from the crystallization conditions was deduced based on the shape and peak height of the $2F_o - F_c$ and $F_o - F_c$ electron density, the potential hydrogen bond interactions and interatomic distances. The crystal structure was refined with three chloride anions, two sodium cations, one glycerol molecule, and 205 water molecules including partial occupancy sites. The final R_{work} (R_{free}) values were 14.7% (19.2%) for all data between 10 and 1.35 Å resolution. The rmsd values from ideal bonds and angles were 0.012 Å and 3.0°. The average *B*-factor for all atoms was 20.9 Å^2; the average *B*-factor for atoms of the inhibitor was 12.7 Å.

Acknowledgment. Financial support by the National Institutes of Health (GM 53386, A.K.G. and GM62920, I.T.W.) is gratefully acknowledged. This work was also supported in part by the Intramural Research Program of the Center for Cancer Research, National Cancer Institute, National Institutes of Health, and in part by a Grant-in-aid for Scientific Research (Priority Areas) from the Ministry of Education, Culture, Sports, Science, and Technology of Japan (Monbu Kagakusho), a Grant for Promotion of AIDS Research from the Ministry of Health, Welfare, and Labor of Japan (Kosei Rohdosho: H15-AIDS-001), and the Grant to the Cooperative Research Project on Clinical and Epidemiological Studies of Emerging and Re emerging Infectious Diseases (Renkei Jigyo: No. 78, Kumamoto University) of Monbu-Kagakusho. The work was supported by the Georgia Research Alliance and the Molecular Basis of Disease program of Georgia State University. We thank Annie Heroux for measuring the X-ray diffraction data at beamline X26C of the National Synchrotron Light Source. Use of the National Synchrotron Light Source, Brookhaven National Laboratory, was supported by the U.S. Department of Energy, Office of Science, Office of Basic Energy Sciences, under Contract No. DE-AC02-98CH10886.

Supporting Information Available: HPLC and HRMS data for compounds **2**−**4**. This material is available free of charge via the Internet at http://pubs.acs.org.

References

(1) United Nations. *2004 Report on the global HIV/AIDS Epidemic: 4th global report*; UN: New York, 2004.
(2) Sepkowitz, K. A. AIDS − the first 20 years. *N. Engl. J. Med.* **2001**, *344*, 1764−1772.
(3) Staszewski, S.; Morales-Ramirez, J.; Tashima, K. T.; Rachlis, A.; Skiest, D.; Stanford, J.; Stryker, R.; Johnson, P.; Labriola, D. F.; Farina, D.; Manion, D. J.; Ruiz, N. M. Efavirenz plus zidovudine and lamivudine, efavirenz plus indinavir, and indinavir plus zidovudine and lamivudine in the treatment of HIV-1 infection in adults. *N. Engl. J. Med.* **1999**, *341*, 1865−1873.
(4) Wainberg, M. A.; Friedland, G. Public health implications of antiretroviral therapy and HIV drug resistance. *J. Am. Med. Assoc.* **1998**, *279*, 1977−1983.
(5) Yoshimura, K.; Kato, R.; Kavlick, M. F.; Nguyen, A.; Maroun, V.; Maeda, K.; Hussain, K. A.; Ghosh, A. K.; Gulnik, S. V.; Erickson, J. W.; Mitsuya, H. A potent human immunodeficiency virus type 1 protease inhibitor, UIC-94003 (TMC-126), and selection of a novel (A28S) mutation in the protease active Site. *J. Virol.* **2002**, *76*, 1349−1358.
(6) Ghosh, A. K.; Pretzer, E.; Cho, H.; Hussain, K. A.; Duzgunes, N. Antiviral activity of UIC−PI, a novel inhibitor of the human immunodeficiency virus type 1 protease. *Antiviral Res.* **2002**, *54*, 29−36.

(7) Koh, Y.; Nakata, H.; Maeda, K.; Ogata, H.; Bilcer, G.; Devasamudram, T.; Kincaid, J. F.; Boross, P.; Wang, Y.-F.; Tie, Y.; Volarath, P.; Gaddis, L.; Harrison, R. W.; Weber, I. T.; Ghosh, A. K.; Mitsuya, H. A novel bis-tetrahydrofuranylurethane-containing non-peptide protease inhibitor (PI) UIC-94017 (TMC-114) potent against multi-PI-resistant HIV In vitro. *Antimicrob. Agents Chemother*. **2003**, *47*, 3123−3129.

(8) Surleraux, D. L. N. G.; Tahri, A.; Verschueren, W. G.; Pille, G. M. E.; de Kock, H. A.; Jonckers, T. H. M.; Peeters, A.; De Meyer, S.; Azijn, H.; Pauwels, R.; de Bethune, M.-P.; King, N. M.; Prabu-Jeyabalan, M.; Schiffer, C. A.; Wigerinck, P. B. T. P. Discovery and selection of TMC114, a next generation of HIV-1 protease inhibitors. *J. Med. Chem.* **2005**, *48*, 1813−1822.

(9) On June 23, 2006, FDA approved new HIV treatment for patients who do not respond to existing drugs. Please see http://www.fda.gov/bbs/topics/NEWS/2006/NEW01395.html.

(10) Tie, Y.; Boross, P. I.; Wang, Y.-F.; Gaddis, L.; Hussain, A. K.; Leshchenko, S.; Ghosh, A. K.; Louis, J. M.; Harrison, R. W.; Weber, I. T. High-resolution crystal structures of HIV-1 protease with a potent non-peptide inhibitor (UIC-94017) active against multi-drug-resistant clinical strains. *J. Mol. Biol.* **2004**, *338*, 341−352.

(11) Hong, L.; Zhang, X.; Hartsuck, J. A.; Tang, J. Crystal structure of an in vivo HIV-1 protease mutant in complex with saquinavir: insights into the mechanisms of drug resistance. *Protein Sci.* **2000**, *9*, 1898−1904.

(12) Laco, G. S.; Schalk-Hihi, C.; Lubkowski, J.; Morris, G.; Zdanov, A.; Olson, A.; Elder, J. H.; Wlodawer, A.; Gustchina, A. Crystal structures of the inactive D30N mutant of feline immunodeficiency virus protease complexed with a substrate and an inhibitor. *Biochemistry* **1997**, *36*, 10696−10708.

(13) Deardorff, D. R.; Windham, C. Q.; Craney, C. L. Enantioselective hydrolysis of *cis*-3,5-diacetoxycyclopentene: (1*R*,4*S*)-(+)-4-hydroxy-2-cyclopentenyl acetate. *Org. Synth.* **1998**, *9*, 487−492.

(14) Busato, S.; Tinembart, O.; Zhang, Z.; Scheffold, R. Vitamin B_{12} a catalyst in the synthesis of prostaglandins. *Tetrahedron* **1990**, *46*, 3155−3166.

(15) Levy, D. E.; Bao. M.; Cherbavaz, D. B.; Tomlinson, J. E.; Sedlock, D. M.; Homcy, C. J.; Scarborough, R. M. Metal coordination-based inhibitors of adenylyl cyclase: novel potent p-site antagonists. *J. Med. Chem.* **2003**, *46*, 2177−2186.

(16) Miyoka, H.; Nagaoka, H.; Okamura, T.; Yamada, Y. A method for synthesizing the diformylcyclopentene moiety of halimedatrial. *Chem. Pharm. Bull.* **1989**, *37*, 2882−2883.

(17) Ghosh, A. K.; Duong, T. T.; McKee, S. P.; Thompson, W. J. *N,N′*-dissuccinimidyl carbonate: a useful reagent for alkoxycarbonylation of amines. *Tetrahedron Lett.* **1992**, *33*, 2781−2784.

(18) The compound **11** can be readily obtained in large quantities from 1,3-cyclooctadiene. See Crandall, J. K.; Chang, L.-H. Base promoted reactions of epoxides: II. 3, 4- and 5,6-epoxycyclooctene. *J. Org. Chem.* **1967**, *32*, 532−536.

(19) Hashimoto, S.; Kase, S.; Shinoda; Tomohiro; Ikegami, S. A regio- and stereocontrolled synthesis of (+)-isocarbacyclin via (1*S*, 2*R*, 5*R*)-bicyclo[3.3.0]oct-6-en-endo-2-ol. *Chem. Lett.* **1989**, 1063−1066.

(20) Shibasaki, M.; Yamazaki, M.; Iseki, K.; Ikegami, S. A simple, highly stereocontrolled total synthesis of (+)-hirustic acid. *Tetrahedron Lett.* **1982**, *23*, 5311−5314.

(21) Corey, E. J.; Venkateswarlu, A. Protection of hydroxyl groups as *tert*-butyldimethylsilyl derivatives. *J. Am. Chem. Soc.* **1972**, *94*, 6190−6191.

(22) Philips, K. D.; Zemilicka, J.; Horowits, J. P. Unsaturated sugars I. Decarboxylative elimination of methyl 2,3-di-*O*-benzyl-α-D-glucopyranosiduronic acid to methyl 2,3-di-*O*-benzyl-4-deoxy-*β*-L-*threo*-pent-4-enopyranoside. *Carbohydr. Res.* **1973**, *30*, 281−286.

(23) Barton, D. H. R.; McCombie, S. W. A new method for the deoxygenation of secondary alcohols. *J. Chem. Soc., Perkin Trans. 1* **1975**, 1574−1585.

(24) Fujita, K.; Hata, K.; Oda, R.; Tabushi, I. Nuclear magnetic resonance studies on cis-bicyclo[3.3.0] oct-7-en-2-yl derivatives. Long-range magnetic anisotropic effect on olefinic protons by the endo-carbonyl group. *J. Org. Chem.* **1973** *38*, 2640−2644.

(25) Ghosh, A. K.; Leshchenko, S.; Noetzel, M. Stereoselective photochemical 1,3-dioxolane addition to 5-alkoxymethyl-2-(5H)-furanone: synthesis of bis-tetrahydrofuranyl ligand for HIV protease inhibitor UIC-94017 (TMC-114). *J. Org. Chem.* **2004**. *69*, 7822−7829.

(26) This sulfonyl chloride was prepared by oxidation of tosyl chloride with CrO_3 in Ac_2O at 0 °C for 1 h (38%).

(27) Toth, M. V.; Marshall, G. R. A simple, continuous fluorometric assay for HIV protease. *Int. J. Pep. Protein Res.* **1990**, *36*, 544−550.

(28) Coordinates and structure factors for the protease-inhibitor **3** complex were deposited in PDB with the accession code 2HB3. For more detailed information, please see the Supporting Information.

(29) Gustchina, A.; Sansom, C.; Prevost, M.; Richelle, J.; Wodak, S. Y.; Wlodawer, A.; Weber, I. T. Energy calculations and analysis of HIV-1 protease-inhibitor crystal structures. *Protein Eng.* **1994**, *7*, 309−317.

(30) Miller, J. F.; Andrews, C. W.; Brieger, M.; Furfine, E. S.; Hale, M. R.; Hanlon, M. H.; Hazen, R. J.; Kaldor, I.; McLean, E. W.; Reynolds, D.; Sammond, D. M.; Spaltenstein, A.; Tung, R.; Turner, E. M.; Xu, R. X.; Sherrill, R. G. Ultra-potent P1 modified arylsulfonamide HIV protease inhibitors: the discovery of GW0385. *Bioorg. Med. Chem. Lett.* **2006**, *16*, 1788−1794.

(31) Clemente, J. C.; Moose, R. E.; Hemrajani, R.; Whitford, L. R.; Govindasamy, L.; Reutzel, R.; McKenna, R.; Agbandje-McKenna, M.; Goodenow, M. M.; Dunn, B. M. Comparing the accumulation of active- and nonactive-site mutations in the HIV-1 protease. *Biochemistry* **2004**, *43*, 12141−12151.

(32) Chen, Z.; Li, Y.; Chen, E.; Hall, D. L.; Darke, P. L.; Culberson, C.; Shafer, J. A.; Kuo, L. C. Crystal structure at 1.9-Å resolution of human immunodeficiency virus (HIV) II protease complexed with L-735, 524, an orally bioavailable inhibitor of the HIV proteases. *J. Biol. Chem.* **1994**, *269*, 26344−26348.

(33) Heaslet, H.; Kutilek, V.; Morris, G. M.; Lin, Y. C.; Elder, J. H.; Torbett, B. E.; Stout, C. D. Structural insights into the mechanisms of drug resistance in HIV-1 protease NL4-3. *J. Mol. Biol.* **2006**, *356*, 967−981.

(34) Martin, J. L.; Begun, J.; Schindeler, A.; Wickramasinghe, W. A.; Alewood, D.; Alewood, P. F.; Bergman, D. A.; Brinkworth, R. I.; Abbenante, G.; March, D. R.; Reid, R. C.; Fairlie, D. P. Molecular recognition of macrocyclic peptidomimetic inhibitors by HIV-1 protease. *Biochemistry* **1999**, *38*, 7978−7988.

(35) Liu, F.; Boross, P. I.; Wang, Y. F.; Tozser, J.; Louis, J. M.; Harrison, R. W.; Weber, I. T. Kinetic, stability, and structural changes in high-resolution crystal structures of HIV-1 protease with drug-resistant mutations L24I, I50V, and G73S. *J. Mol. Biol.* **2005**, *354*, 789−800.

(36) Logsdon, B. C.; Vickrey, J. F.; Martin, P.; Proteasa, G.; Koepke, J. I.; Terlecky, S. R.; Wawrzak, Z.; Winters, M. A.; Merigan, T. C.; Kovari, L. C. Crystal structures of a multidrug-resistant human immunodeficiency virus type 1 protease reveal an expanded active-site cavity. *J. Virol.* **2004**, *78*, 3123−3132.

(37) Martin, P.; Vickrey, J. F.; Proteasa, G.; Jimenez, Y. L.; Wawrzak, Z.; Winters, M. A.; Merigan, T. C.; Kovari, L. C. "Wide-open" 1.3 Å structure of a multidrug-resistant HIV-1 protease as a drug target. *Structure* **2005**, *13*, 1887−1895.

(38) Curran, T. T.; Hay, D. A. Resolution of *cis*-4-*O*-TBS-2-cylopenten-1,4-diol. *Tetrahedron: Asymmetry* **1996**, *7*, 2791.

(39) Otwinowski, Z.; Minor, W. Processing of X-ray diffraction data in oscillation mode. *Met. Enzymol.* **1977**, *1276*, 307−326.

(40) Collaborative Computational Project, Number 4 The CCP4 Suite: Programs for Protein Crystallography. *Acta Crystallogr.* **1994**, *D50*, 760−763.

(41) Potterton, E.; Briggs, P.; Turkenburg, M.; Dodson, E. A graphical user interface to the CCP4 program suite. *Acta Crystallogr.* **2003**, *D59*, 1131−1137.

(42) Sheldrick, G. M.; Schneider, T. R. High-resolution refinement. *Met. Enzymol.* **1997**, *277*, 319−343.

(43) Jones, T. A.; Zou, J. Y.; Cowan, S. W.; Kjeldgaard, M. Improved methods for building protein models in electron density maps and the location of errors in these models. *Acta Crystallog.* **1991**, *A47*, 110−119.

JM060561M